ISTFA™ 2018: Conference Proceedings from the 44th
International Symposium for Testing and Failure Analysis
October 28–November 1, 2018, Phoenix, Arizona, USA

Narrow-Beam Argon Ion Milling of Ex Situ Lift-Out FIB Specimens Mounted on Various Carbon-Supported Grids

M. J. Campin, C. S. Bonifacio, P. Nowakowski, and P. E. Fischione
E.A. Fischione Instruments, Inc., Export, PA 15632 USA

L. A. Giannuzzi
EXpressLO LLC, Lehigh Acres, FL 33971 USA

Abstract

The semiconductor industry recently has been investigating new specimen preparation methods that can improve throughput while maintaining quality. The result has been a combination of focused ion beam (FIB) preparation and ex situ lift-out (EXLO) techniques. Unfortunately, the carbon support on the EXLO grid presents problems if the lamella needs to be thinned once it is on the grid. In this paper, we show how low-energy (< 1 keV), narrow-beam (< 1 μm diameter) Ar ion milling can be used to thin specimens and remove gallium from EXLO FIB specimens mounted on various support grids.

Introduction

FIB tools are commonly used to prepare site-specific transmission electron microscopy (TEM) specimens due to the accuracy and repeatability of specimen thinning and extraction that it provides [1]. In addition, the EXLO method of preparing TEM specimens is increasingly employed, particularly by the semiconductor industry, with the goal of increasing throughput [2-3]. Currently, there are two main types of carbon-supported grids used by the semiconductor industry for EXLO specimen preparation: standard mesh grids and perforated grids. Standard carbon-supported mesh grids are cheaper and only require that the TEM specimen be placed somewhere on the carbon support within one of the grid openings. However, because the carbon support film is continuous across the entire grid, milling can only be done from one side of the lamella. Because of this, surface damage and Ga implantation caused during FIB milling can be removed from one side of the lamella, but not the other; this may impact the ability to perform high-resolution TEM (HRTEM) imaging and analysis. In contrast, perforated, carbon-supported, mesh-type grids require precise positioning of the lamella over one of the perforations in the carbon support, but allow for removal of surface damage and Ga implantation from both sides of the lamella. This is the best possible scenario for obtaining high quality HRTEM imaging and analysis.

When performing HRTEM characterization and failure analysis of materials and devices, it is necessary to create very thin, defect-free TEM lamellae containing the features of interest. If the spatial location of features is not precisely known, as is often the case when performing root-cause failure analysis or investigating processing defects, the lamella may require iterative thinning steps. Additional thinning of TEM lamellae prepared using in situ methods can easily be performed. In contrast, further thinning of the TEM specimen mounted on a thin carbon support with a Ga ion beam is limited due to the rapid, deleterious milling of the carbon support, which can result in the loss of the specimen.

Ga ion milling is known to cause artifacts, such as surface damage and ion-implanted layers, which limit analytical and high-resolution electron microscopy. In contrast, low energy (< 1 keV) Ar ion milling has been shown to improve specimen quality [4-7]. In addition, low energy Ar ion milling allows for precise milling and endpointing [8].

In this paper, we demonstrate the ability of low energy (<1 keV), narrow-beam (<1 μm diameter) Ar ion milling to thin and improve specimen quality of carbon-supported EXLO specimens, including the reduction of both curtaining and Ga implantation.

Discussion

EXLO TEM specimens from patterned semiconductor wafers were FIB-prepared and transferred to either holey carbon-supported mesh grids or perforated carbon-supported, mesh-type grids. In this work, the FIB milling direction was from the top of the lamellae and parallel to the vertical airgap structures. TEM lamellae with an expected thickness of > 100 nm at the area of interest were produced. The lamellae were mounted using standard EXLO methods so that the lamella was located near the center of the grid square (Figure 1a) and, in the case of perforated, carbon-supported grids, with the area of interest positioned directly over a hole in the carbon support (Figure 1b). Narrow-beam Ar ion milling was performed using the PicoMill® TEM specimen preparation system [Fischione Instruments], which rasters the ion beam within a milling box placed over the area of interest. Because milling with varying

incident angles has been shown to reduce curtaining, we chose to orient the specimens so that the Ar ion beam milling direction was at an angle compared to the FIB milling direction [9-10]. TEM imaging was then used to evaluate improvement in specimen quality, energy-filtered TEM (EFTEM) imaging was used to quantify the reduction in thickness, and energy-dispersive X-ray spectroscopy (EDS) was used to quantify reduction in Ga implantation.

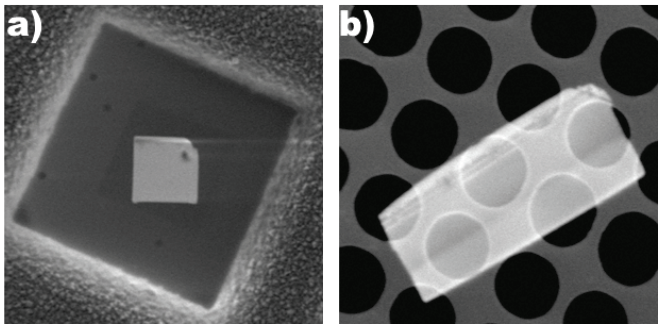

Figure 1: PicoMill system SED images of TEM lamellae mounted on mesh grids with holey carbon support (left) and perforated carbon support (right).

In Situ Imaging During Milling

The PicoMill system has both an electron column for SEM imaging and an Ar ion beam column for imaging and milling. Its < 1 µm beam size, capability to precisely position the ion beam, and low current densities make it possible to thin lamella with minimal damage to the supporting carbon foil [7]. In addition, it has both a secondary electron detector (SED) and a bright-field scanning transmission electron microscopy (STEM) detector. The live imaging capability of the integrated SED and STEM detectors enables the tracking of both specimen and carbon support thickness reduction during milling by measuring changes in image contrast [8].

Milling of EXLO TEM Specimens Mounted on Continuous Carbon-Supported Grids

A TEM specimen mounted in the center of a continuous holey carbon-supported grid square was selected for milling. In addition, the grid was rotated such that the Ar ion milling direction was from the side of the lamella (~90˚ rotationally offset from the FIB milling direction). For each milling step, a 10 x 10 μm^2 milling box was placed over the lamella in the SED image. Initial milling was performed from the side of the grid on which the lamella was mounted using a 700 eV Ar ion beam with 90 pA current. Live imaging using the integrated SED and STEM detectors was done while milling to prevent milling away all of the carbon support. Additional milling was performed using a 500 eV beam with 90 pA current to clean up the lamella surface. In situ SED and STEM images acquired in the PicoMill system before and after ion milling show removal of some of the supporting carbon film adjacent to the TEM lamella, but that the lamella remained intact after milling (Figure 2).

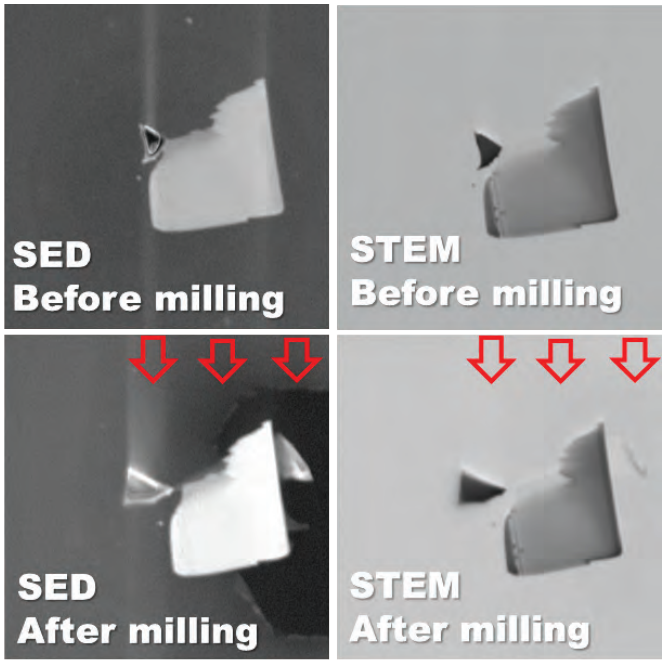

Figure 2: In situ SED and STEM images of a TEM lamella mounted on holey carbon support acquired in the PicoMill system before and after milling. Red arrows indicate the milling direction. The lamella was milled using a 700 eV beam with 90 pA current for 6 minutes followed by milling with a 500 eV beam with 90 pA current for 10 minutes.

TEM imaging and analysis was performed using a Tecnai TF30 TEM [Thermo Fisher Scientific] with GIF2001 [Gatan] and EDS [EDAX] system. TEM images acquired before and after milling show removal of sputtered material and reduction of curtaining (Figure 3). In addition, the TEM images show the ability to resolve distinct features within the lamella which were indistinguishable before milling (Figure 4). Finally, EFTEM thickness maps acquired before and after milling confirm a reduction in specimen thickness (Figure 5).

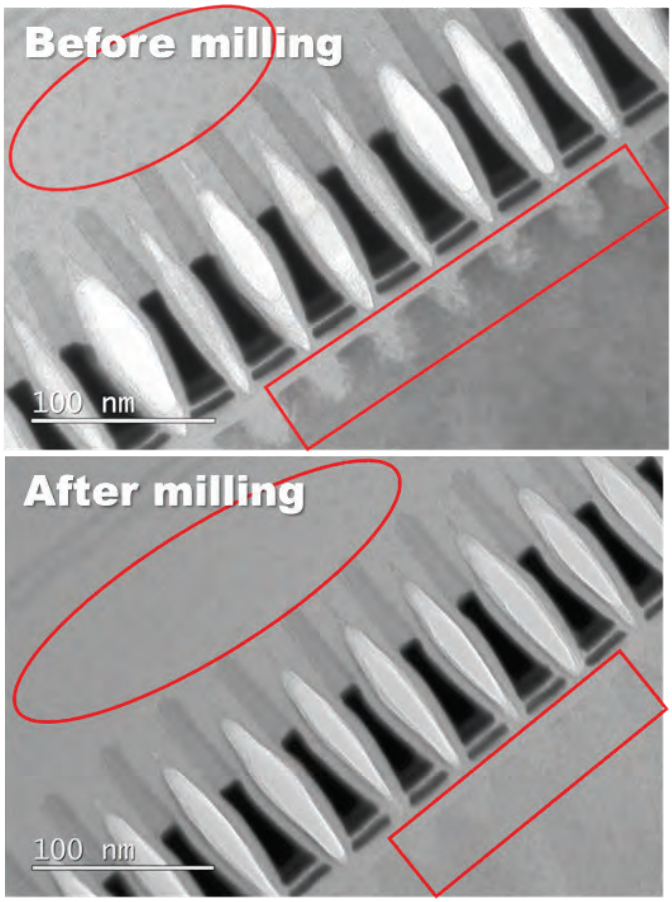

Figure 3: TEM images acquired before and after ion milling of a TEM lamella on a holey carbon support grid show the removal of sputtered material above the gates (red circle) and the reduction of curtaining in the silicon below the gates (red rectangle) after ion milling.

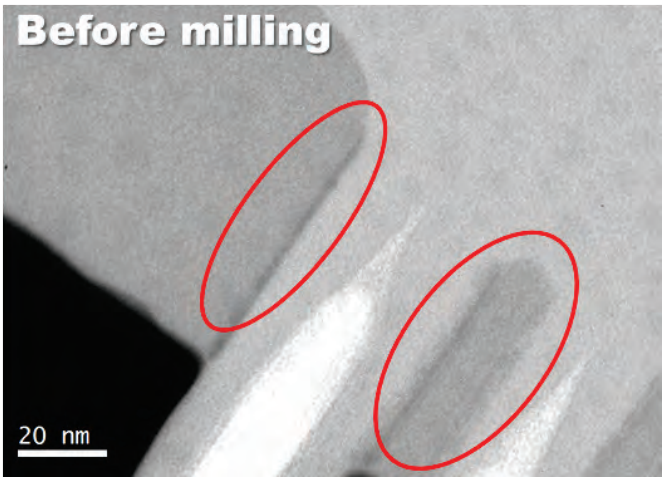

Figure 4: HRTEM images acquired before and after ion milling of a TEM lamella on a holey carbon support grid show the ability to resolve distinct features/layers within the lamella which were indistinguishable before milling.

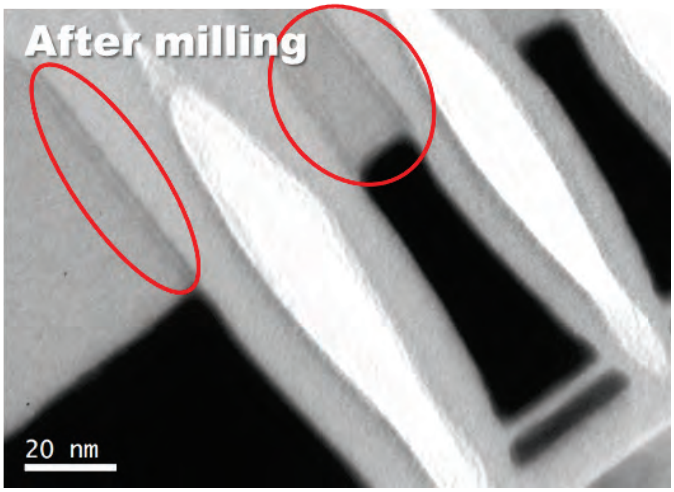

Figure 4 (continued): HRTEM images acquired before and after ion milling of a TEM lamella on a holey carbon support grid show the ability to resolve distinct features/layers within the lamella which were indistinguishable before milling.

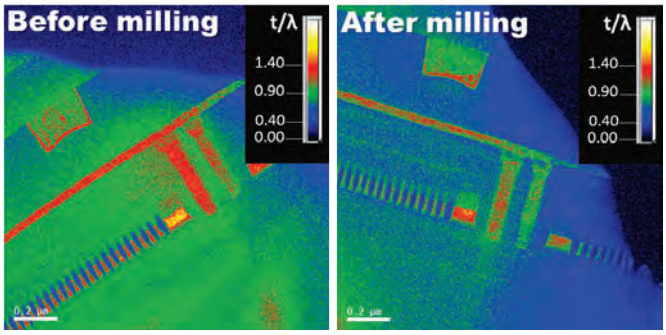

Figure 5: EFTEM thickness maps acquired before and after ion milling show a reduction in specimen thickness after ion milling.

Milling of EXLO TEM Specimens Mounted on Perforated, Carbon-Supported Grids

Attaching TEM specimens to perforated, carbon-supported, mesh-type grids is a common EXLO method used by the semiconductor industry [4]. For this reason, we selected a TEM specimen which was mounted over several holes in the center of a square on a perforated, carbon-supported, mesh-type grid for our milling experiments. Milling was performed from both sides of the grid using a 700 eV Ar ion beam with 90 pA current. In addition, the grid was rotated such that the Ar ion milling direction was from the top right of the lamella (~45˚ rotationally offset from the FIB milling direction). As was done in the previous milling experiments, a 10 x 10 μm^2 milling box was placed directly over the lamella in the SED image and live imaging with the integrated SED and STEM detectors was done to track the degree of carbon support milling. In situ SED and STEM images acquired in the PicoMill system before and after ion milling show removal of some of the carbon support; however, the lamella remained intact after milling (Figure 6).

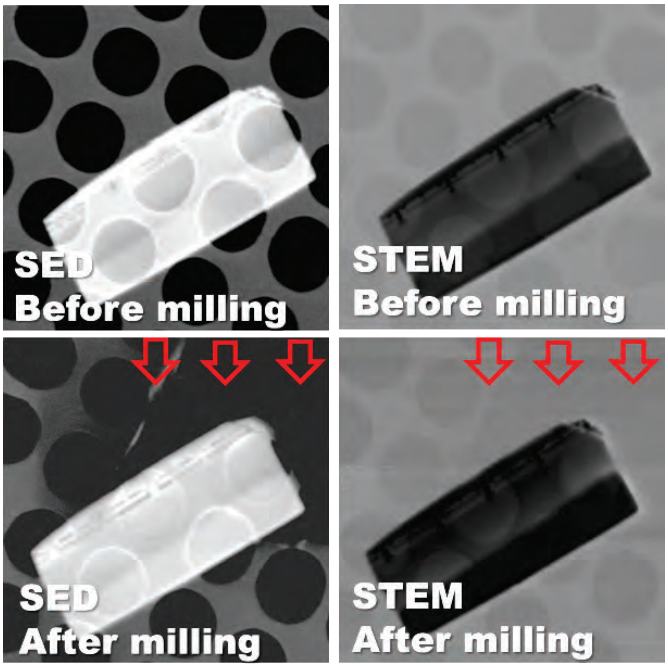

Figure 6: In situ SED and STEM images of a TEM lamella mounted on a perforated carbon support grid acquired in the PicoMill system before and after milling. Red arrows indicate the milling direction. The lamella was milled using a 700 eV beam with 90 pA current for 17 minutes.

TEM images acquired before and after milling show removal of sputtered material and reduction of curtaining (Figure 7). In addition, the TEM images show the ability to resolve distinct features within the lamella which were indistinguishable before milling (Figure 8). Finally, EFTEM thickness maps acquired before and after milling confirm a reduction in specimen thickness (Figure 9).

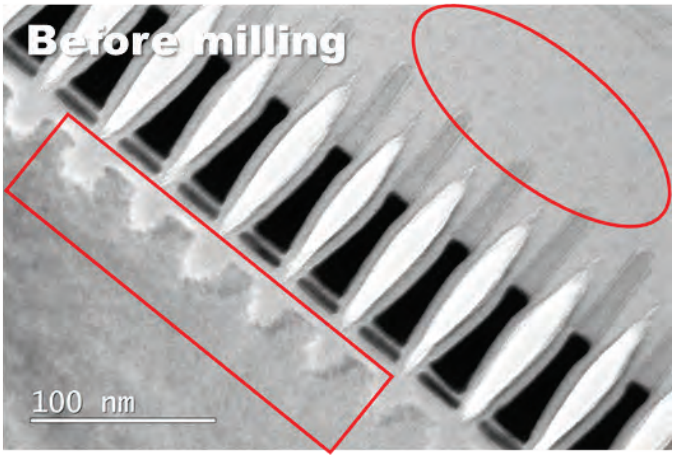

Figure 7: TEM images acquired before and after ion milling of a TEM lamella on a perforated carbon support grid show removal of sputtered material above the gates (red circle) and reduction of curtaining in the silicon below the gates (red rectangle) after ion milling.

Figure 7 (continued): TEM images acquired before and after ion milling of a TEM lamella on a perforated carbon support grid show removal of sputtered material above the gates (red circle) and reduction of curtaining in the silicon below the gates (red rectangle) after ion milling.

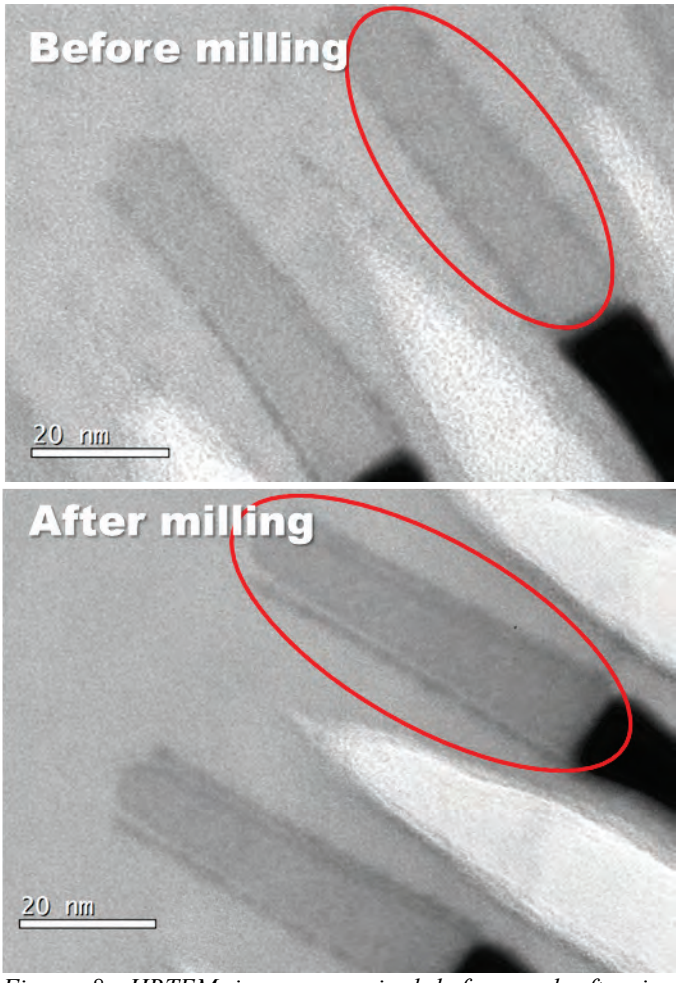

Figure 8: HRTEM images acquired before and after ion milling of a TEM lamella on a perforated carbon support grid show the ability to resolve distinct features/layers within the lamella which were indistinguishable before milling.

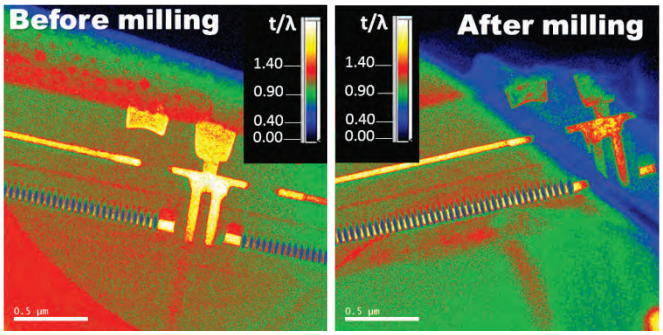

Figure 9: EFTEM thickness maps acquired before and after ion milling show a reduction in specimen thickness after ion milling.

Gallium Reduction after PicoMilling

Ga ions used in FIB tools are known to implant gallium ions into the specimen surface, which can negatively affect HRTEM imaging and analysis [2]. To remove the gallium implanted layers, it is necessary to mill the lamella surfaces using non-reactive ion species. In this experiment, we also had the additional restriction that we wanted to minimize the milling of the carbon support. This was accomplished using the PicoMill system's low energy (< 1 keV), narrow Ar ion beam (< 1 µm diameter).

To verify the ability of the PicoMill system to remove gallium, EDS was performed on a TEM lamella before and after milling. A high angle annular dark field (HAADF) STEM image showing the placement of a 20 nm x 50 nm EDS acquisition box in the area of interest is shown in Figure 10. Identical experimental conditions were used for EDS spectra acquisition before and after milling: 10 degree tilt towards the EDS detector, a probe size of ~0.5 nm, 5 eV/ch. dispersion, 17 µs dwell time and 30 second live time. The EDS spectra show that the Ga signal was slightly reduced after milling (Figure 10). However, while it is possible to reduce the amount of Ga in the TEM lamella, due to the short milling times it is unlikely that all of the Ga will be removed before the carbon support becomes compromised. It is therefore advisable to use as low of kV as possible for the low kV cleaning step in the FIB in order to minimize the amount of Ga implantation before placing the specimen on a carbon supported grid.

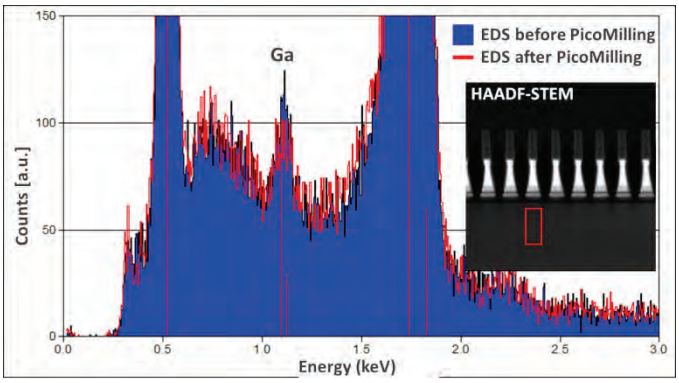

Figure 10: EDS spectra acquired before and after ion milling show a reduction in Ga after ion milling. The HAADF-STEM image (inset) shows the area from which the EDS spectra were acquired.

Conclusions

It is possible to thin a TEM lamella mounted on a mesh-type TEM grid with thin carbon support or on a perforated, carbon-supported, mesh-type TEM grid using the PicoMill system. For the former, milling was performed on one side of the specimen, and for the latter, milling was performed on both sides of the specimen. In both cases, the low current densities of the Ar ion beam allowed thinning of the lamella with minimal damage to the supporting grid. This allows thinning of the targeted area, removal of sputtered material, reduction of curtaining and the ability to resolve distinct features within the lamella which were indistinguishable before milling.

References

[1] Giannuzzi, L. A., and Stevie, F. A., "A review of focused ion beam milling techniques for TEM specimen preparation," *Micron*, Vol. 30, No. 3 (1999), pp. 197-204.

[2] Mayer, J., Giannuzzi, L. A., Kamino, T., Michael, J., "TEM sample preparation and FIB-induced damage," *MRS Bull.*, Vol. 32, No. 5 (2007), pp. 400-407.

[3] Giannuzzi, L. A., Yu, Z., Yin, D., Harmer, M. P., Xu, Q., Smith, N. S., Chan, L., et al., "Theory and new applications of ex situ lift out," *Microsc. Microanal.*, Vol. 21, No. 4 (2015), pp. 1034-1048.

[4] Kang, H. H., King, J. F., Patterson, O. D., Herschbein, S. B., Nadeau, J. P., Fuller, S. E., "High volume and fast turnaround automated inline TEM sample preparation for manufacturing process monitoring," *Proc 33rd Int'l Symp for Testing and Failure Analysis,* Dallas, TX, November 2010, pp. 102-107.

[5] Unocic, K. A., Mills, M. J., Daehn, G. S., "Effect of gallium focused ion beam milling on preparation of aluminium thin foils," *J. Microsc.*, Vol. 240, No. 3 (2010), pp. 227-238.

[6] Cerchiara, R. R., Fischione, P. E., Liu, J., Matesa, J. M., Robins, A. C., Fraser, H. L., Genç, A., "Raising the standard of specimen preparation for aberration-corrected TEM and STEM," *Microsc. Today*, Vol. 19, No. 1 (2011), pp. 16-19.

[7] Nowakowski, P. et al., "Accurate removal of implanted gallium and amorphous damage from TEM specimens after FIB preparation", *Microsc. Microanal.* Vol. 23 (2017), pp. 300-301.

[8] Bonifacio, C.S. et al., "Automated end-point detection and targeted Ar^+ milling of advanced integrated circuit FIB TEM specimens," *Proc. 43rd Int'l Symp for Testing and Failure Analysis*, Pasadena, CA, November 2017, pp. 394-398.

[9] Denisyuk, A. et al., "Mitigating curtaining artifacts during Ga FIB TEM lamella preparation of a 14 nm FinFET device," *Microsc. Microanal.* Vol. **23**, Issue 3 (2017), pp. 484-490.

[10] Montoya, E. et al., "Evaluation of top, angle, and side cleaned FIB Samples for TEM analysis," *Microsc. Res. and Tech.* **70** (2007) 1060-1071.